

### 6.3. RHIC 130 mm Aperture Interaction Region Quadrupole Cross-section

A total of seventy two, 130 mm aperture quadrupoles are required in six interaction regions of RHIC. Each interaction region includes 4 sets of quadrupole triplets (see Fig. 5.2.11 which shows one of two beam lines at an intersection). The Q1, Q2 and Q3 quadrupoles in each triplet have the same cross section, and magnetic lengths, respectively, of 1.44 m, 3.4 m and 2.1 m. The major parameters of these quadrupoles are shown in Table 6.3.1.

The particle beam is focussed to a small size at the crossing point in the two low-beta ( $\beta^*=1$ ) interaction regions to obtain a high luminosity. An unavoidable consequence of this squeeze is the increase in the beam size in these quadrupoles. Moreover, the rapid variation in beam size within the focusing triplet limits the effectiveness of the local and lumped global corrector system [171]. Therefore, good field quality in these quadrupoles is crucial to the high luminosity operation of RHIC. Since the maximum luminosity is desired at the top energy, the field errors are designed to be minimized at the maximum operating gradient.

#### 6.3.1. Basic Construction

The cross section of the cold mass is shown in Fig. 6.3.1. Following the design philosophy used in most other RHIC magnets, the yoke is used here as a collar to compress the coils. The yoke aperture consists of concentric circular arcs with two radii instead of the usual circular aperture. As explained in chapter 2, this reduces the  $b_5$  saturation by over an order of magnitude. The space between the coil and the yoke is filled with a thin, glass-filled phenolic spacer. The spacer has two radii for the outer surface which closely follows the geometry of the yoke inner surface. However, at eight places a gap is left between the yoke and spacer where partially magnetic tuning shims are placed to correct the measured field harmonics after the coils are assembled in the yoke. The tuning shims are discussed in more detail in a previous chapter. A 6.35 mm thick stainless steel shell enclosing the yoke is welded together after the collaring keys are inserted in the compressed yoke. The quadrupoles of the inner and outer rings share a common cryostat. The minimum center-to-center distance between adjacent Q1 quadrupoles is 424 mm.



**Table 6.3.1:** The basic design parameters of the 130 mm aperture quadrupoles for the RHIC interaction regions.

Parameter	Value
Superconducting wire diameter . . . .	0.65 mm
Number of wires per cable . . . . .	36
Copper to superconductor ratio . . . .	1.8
Cable mid-thickness . . . . .	1.16 mm
Cable width . . . . .	11.7 mm
Cable insulation . . . . .	Kapton CI
Critical current at 5.6T, 4.2 K . . . .	$\geq 10100$ A
Number of turns per pole . . . . .	27
Coil inner radius . . . . .	65 mm
Coil outer radius . . . . .	77 mm
Yoke lamination thickness . . . . .	6.35 mm
Yoke inner radius at midplane . . . .	87 mm
Yoke inner radius at pole . . . . .	92 mm
Yoke outer radius . . . . .	175.26 mm
Magnetic length, Q1, Q2, Q3 . . . .	1.44, 3.4, 2.1 m
Stored energy in Q2 magnet . . . . .	165 kJ
Minimum beam spacing in triplet ..	424 mm
Maximum design current . . . . .	5.05 kA
Maximum design gradient . . . . .	48.1 T/m
Operating temperature . . . . .	4.6 K
Computed quench current at 4.6 K	8.26 kA
Computed quench gradient at 4.6 K	75.3 T/m
Gradient margin . . . . .	57%

**Table 6.3.2:** The basic coil design parameters of the 130 mm aperture quadrupoles for the RHIC intersection regions. The harmonics  $b_n$  for the final cross section are given at 40 mm reference radius. “Circular iron aperture” rows show the expected harmonics for a circular iron aperture with a yoke inner radius of 87 mm. “Actual iron aperture” rows show the expected harmonics for the two radii (87 mm and 92 mm) design. The table also includes the harmonics due to nominal tuning shims and the effect of the asymmetric deformation in the yoke aperture during collaring.

Parameter	Value
Number of layer(s) .....	1
Number of wedges .....	2
Turn configuration (from midplane) .	13, 8, 6
Wedge 1, Min./Max. thickness, mm .	1.143/1.143
Wedge 2, Min./Max. thickness, mm .	4.227/6.35
Coil-to-midplane gap (0°, 180°), mm .	0.356 mm
Coil-to-midplane gap (90°, 270°), mm	0.279 mm
Coil inner radius .....	65 mm
Coil outer radius .....	77 mm
$b_3$ for circular iron aperture .....	3.0
$b_3$ for actual iron aperture .....	0.0
$b_5$ for circular iron aperture .....	-29.6
$b_5$ for actual iron aperture .....	-1.2
$b_7$ for circular iron aperture .....	-0.22
$b_7$ for actual iron aperture .....	-0.1
$b_9$ for circular iron aperture .....	1.1
$b_9$ for actual iron aperture .....	0.0

### 6.3.2. Coil Cross Section

One octant of the coil cross section is shown in Fig. 6.3.2. The coil has a total of 27 cables per octant in three blocks. The coil is designed using a superconducting cable which is used in the outer layer of the SSC 50 mm dipole magnet (see Table 6.2.1). This cable is

$\sim 20\%$  wider than the one which is used in the RHIC arc dipole and quadrupole magnets. The additional superconductor in this wider cable gave a sufficient margin over the original design gradient of 59 T/m in a single layer coil. As shown, in Table 6.3.1, the design gradient in the present RHIC lattice has been reduced to 48.1 T/m. The specifications for the critical current  $I_c$  at 4.2 K and at 5.6 T in wire and in cable are respectively 286 A and 10100 A. The cable is almost fully keystoneed for the 130 mm coil aperture.

The coil is optimized using the computer program PAR2DOPT [130]. This is an analytic program which computes and optimizes field harmonics for a coil in a circular iron aperture. As mentioned earlier, the iron aperture is not circular in this design. This means that a coil optimized for zero harmonics in a circular aperture would have non-zero harmonics here. Therefore, the coil is designed with non-zero harmonics in a circular aperture to cancel the harmonics generated by this non-circular iron aperture. These required non-zero values (also referred to as offsets) are computed using the code POISSON.

The optimized coil cross section is shown in Fig. 6.3.2. The coil has 27 turns in the three blocks (two wedges) of each octant with the distribution of the number of turns in the three blocks being 13, 8 and 6. The two wedges are mechanically symmetric. In addition, the smaller wedge (the one which is closer to the midplane) is rectangular. The various mechanical and magnetic parameters of this cross section are shown in Table 6.3.2. The presence of  $b_3$  and  $b_7$ , which are normally non-allowed harmonics in quadrupoles, is discussed later. In addition to low harmonic content and a lower value of maximum field on the conductor, this particular cross section was chosen for its good flexibility (tunability) in accommodating changes in field harmonics and mechanical parameters such as the thickness of the cable.

The good tunability of coil cross section and the one rectangular wedge turned out to be very useful in obtaining a good field quality in pre-production model magnets when a decision to change the cable insulation was made. The new Kapton-CI insulation increased the thickness of the insulated cable by 0.023 mm compared to the original design. This would have resulted in an 0.635 mm increase in coil size since there are 27 turns in the cross section. This is about an order of magnitude more than the tolerance required to maintain the desired pre-compression on the coils. However, since the shape of one of the wedges was rectangular, it could be easily rolled to a 0.635 mm smaller size. This reduction in wedge size compensated for the thicker insulation, and the original coil size and coil pole angle in the magnet could be maintained. This avoided an adjustment in the number of

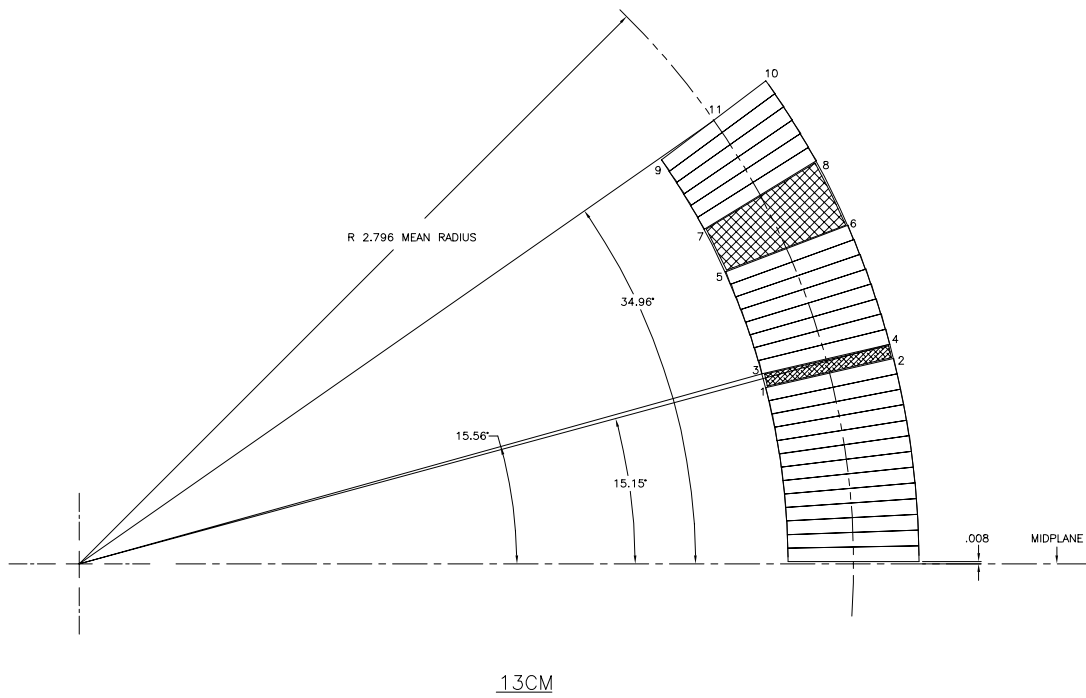


**Figure 6.3.2:** Optimized coil cross section for the RHIC 130 mm aperture insertion quadrupole.

parts in the body and the end section of the magnet. In this selected cross section, the above change did not produce a significant change in  $b_5$ , the first allowed harmonic with quadrupole symmetry. This straightforward accommodation of a large mechanical change without a corresponding deterioration in the field quality was possible only because the cross section was optimised and chosen to permit such tunability. The value of the next allowed harmonic  $b_9$ , created by the large change, is about 1 unit. This was removed in the next iteration.

In an attempt to maximize the use of existing tooling, these quadrupoles are collared like dipoles. However, during the collaring an elliptical deformation is created in the iron and also in the coil since the yoke inner surface defines the coil outer surface. The turns on the horizontal axis are displaced inward and an overall ovality is created as the vertical axis tends to elongate. This deformation breaks an ideal quadrupole symmetry and creates the non-allowed harmonics  $b_3$ ,  $b_7$ , etc. A large value ( $\sim 6$  unit) of  $b_3$  harmonic was observed in the pre-production quadrupoles due to this yoke deformation (asymmetry). A method was developed to remove the harmonics created by this asymmetry. A deliberate difference between the horizontal and vertical midplane gap (see Table 6.3.2) in the coil cross section was introduced. This difference in midplane gap breaks the horizontal/vertical symmetry in the coil cross section and generates the harmonics  $b_3$ ,  $b_7$ , etc. The amount of this second asymmetry (coil asymmetry) can be adjusted to properly compensate for the first asymmetry (yoke asymmetry) created in the collaring press. The calculations and measurements showed that if the half-gap on the horizontal midplane is made about 0.1 mm larger than the half-gap on the vertical midplane, then the  $b_3$  due to yoke asymmetry can be compensated. This was incorporated in eight quadrupoles. However, the asymmetry in coil assembly also produces a small (-0.35 unit) but significant  $b_7$ . Therefore, in later magnets, only part of the correction is applied using this method. The rest is obtained using magnetic tuning shims. The sign of  $b_3$  and  $b_7$  in the two methods is opposite. Therefore, in principle when an asymmetric midplane shim is used in conjunction with the magnetic tuning shims, both  $b_3$  and  $b_7$  could be made zero. However, that would take away a significant part of the tuning shim capacity which could be used to compensate other harmonics. In the final design the target  $b_3$  is zero and  $b_7$  is about -0.1 unit.

### 6.3.3. Yoke Cross Section

In cosine  $\theta$  magnets, the iron aperture is circular. However, in order to reduce the  $b_5$  due to saturation the conventional circular shape has been modified in this design. The yoke aperture is defined by arcs of two concentric circles having radii of 87 mm at the midplane and 92 mm at the pole. This method has been very effective in reducing the  $b_5$  due to saturation from 15 to 1 unit. The basic principle behind it is that it forces an early saturation at the yoke midplane (unless the yoke outer diameter is too large) and delays/reduces the saturation at the pole. Saturation control holes which were found very effective in dipoles are not so effective in the quadrupoles. The nominal transition from 87 to 92 mm occurs at about 30 degrees in the first octant (the angle in the other octants is defined by quadrupole symmetry). At  $\theta = 30$  degree (and similarly in other octants) there is a straight face perpendicular to the midplane, extending from the smaller yoke radius of 87 mm to the larger iron radius of 92 mm. The position angle and the difference between these two radii are used as parameters in the optimization process to reduce the  $b_5$  saturation. The size of the locating notch, shown in Fig. 6.3.1, at the midplane of the yoke aperture is 5 mm deep and 10 mm wide. Four slots – two for helium bypass and two for bus work – are located symmetrically at  $45^\circ$ ,  $135^\circ$ ,  $225^\circ$  and  $315^\circ$  as shown in the figure. The size, shape and location of these slots are determined by the magnetic, mechanical and cooling requirements. Other structures in the yoke are also shown in the figure. Though several of these structures break a strict 8-fold quadrupole symmetry, their location is such that their influence on the iron saturation is minimal. These structures include the holes in the yoke for the stainless steel (non-magnetic) pins and and cutouts for the stainless steel keys. The results of computer calculations show that these holes and cutouts in the yoke generate symmetry breaking harmonics of less than 0.1 unit in the design range of operation. The presence of another quadrupole in the other ring may influence the field at the center of the magnet at high currents. This would be a maximum when the separation between the two magnets is a minimum. Moreover, it is maximum when both of these magnets run at the same high gradient. Computer calculations show that these cross talk induced harmonics are less than 0.1 unit.

The calculations have been performed using the computer codes POISSON, PE2D and MDP. Good agreement has been found between the results obtained by these three codes; this is important because the yoke saturation has been significantly altered in this design by the 2-radius aperture. A computer model of one quadrant of the magnet for the code



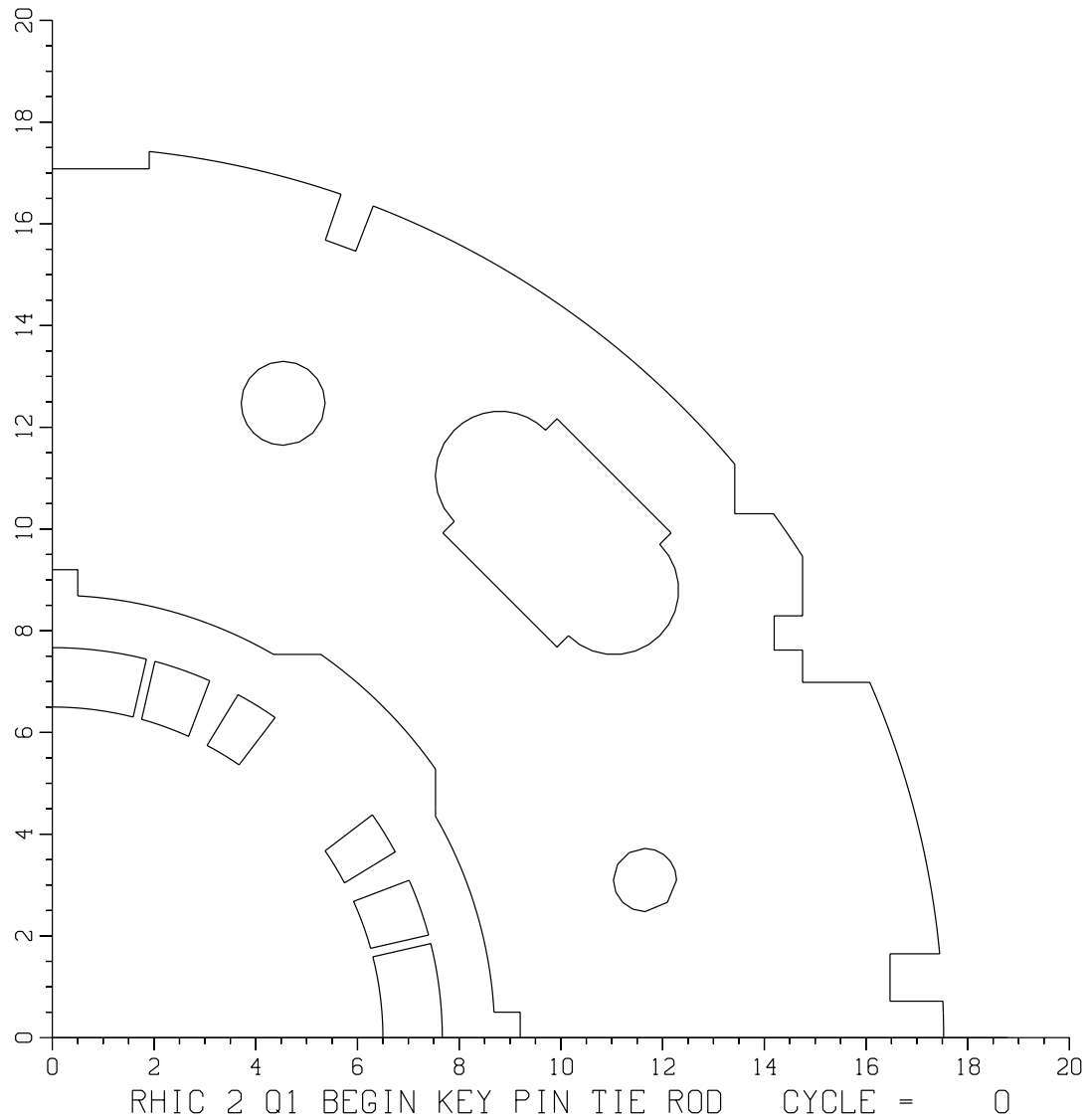


**Figure 6.3.3:** POISSON model for 1/4 of the cold mass cross section of the RHIC 130 mm aperture insertion quadrupole. The rest of the cold mass is described by the symmetry. A perfect quadrupole has an eight fold symmetry; this is partly broken here by the yoke split on the horizontal midplane.

**Table 6.3.3:** Harmonics in the straight section of the RHIC 130 mm aperture insertion quadrupoles as computed for a POISSON model of a quadrant of the magnet. The harmonics are given at 40 mm radius.  $\infty\mu$  represents the calculations when the permeability in the iron is assumed to be  $\infty$ . *Grad* denotes the field gradient. A dependence of the harmonics  $b_3$  and  $b_7$  on the current reflects the absence of an ideal 8-fold quadrupole symmetry.

I	<i>Grad</i>	T.F.	$b_3$	$b_5$	$b_7$	$b_9$	$b_{11}$	$b_{13}$
kA	T/m	T/m/kA	$10^{-4}$	$10^{-4}$	$10^{-4}$	$10^{-4}$	$10^{-4}$	$10^{-4}$
$\infty\mu$	$\infty\mu$	9.574	0.00	-1.20	0.00	-0.10	0.00	0.0
1.0	9.5730	9.573	0.00	-1.22	0.00	-0.10	0.00	0.00
3.0	28.7165	9.5722	0.00	-1.23	0.00	-0.10	0.00	0.00
4.0	38.2583	9.5646	0.03	-1.16	-0.01	-0.05	-0.01	0.00
5.0	47.6639	9.5328	0.10	-1.11	0.00	0.13	-0.01	-0.01
5.5	52.2567	9.5012	0.15	-1.28	-0.01	0.26	0.00	-0.01
6.0	56.7096	9.4516	0.10	-1.36	-0.02	0.39	0.00	-0.01
6.5	60.9980	9.3843	0.08	-1.32	-0.03	0.52	0.00	-0.01
7.0	65.1189	9.3027	0.04	-1.58	-0.04	0.63	-0.01	-0.01
7.5	69.0485	9.2065	0.02	-2.40	-0.05	0.72	-0.01	0.00
8.0	72.8282	9.1035	-0.11	-3.70	-0.07	0.78	-0.01	0.00
8.5	76.5207	9.0024	-0.40	-5.21	-0.09	0.83	-0.01	0.01
9.0	80.1618	8.9069	-0.65	-6.76	-0.10	0.86	-0.01	0.01
9.5	83.7541	8.8162	-0.76	-8.30	-0.11	0.88	-0.01	0.02

POISSON is shown in Fig. 6.3.3. The results of calculations showing the current dependence of the harmonics allowed by the actual geometry are given in Table 6.3.3. The harmonics  $b_3$ ,  $b_7$  and  $b_{11}$  are not allowed in a strictly 8-fold quadrupole symmetry. The dependence of them on current reflects the absence of the ideal 8-fold symmetry. The yoke is designed such that the magnitude of these harmonics is small even at high currents. The computed dependence of the harmonics  $b_3$ ,  $b_5$  and  $b_9$  on current is plotted in Fig. 6.3.4.

The calculations described above are for one magnet by itself, i.e. no other magnet is present in the vicinity. However, in the layout of the RHIC lattice, there is always another 130 mm aperture quadrupole located nearby. The minimum separation between the outer yoke diameter of the two is  $\sim 73.5$  mm. The thickness of the iron yoke in these quadrupoles, though sufficient to contain the field lines at the design current, is not sufficient to contain them at the quench current of 8.26 kA. In this situation, the non-allowed harmonics show a dependence on current at high field. This is commonly referred to as cross talk and it implies that the field of one magnet is influencing the field in the aperture of the other magnet.

In RHIC, the ratio of rigidities of the two counter rotating beams varies in the range of 1:1 to 1:0.4. That means that the excitation of two side-by-side quadrupoles can, in general, be different. The direction of the field in the two is the same. In this case, the amount of cross talk between the two quadrupoles is a maximum when both are excited at the same high current (1:1 case). Therefore, in the calculations presented here for the non-allowed field harmonics, only the 1:1 case is considered. The cross talk is a maximum at the Q1 location where the two quadrupoles are at their minimum separation, with a center-to-center distance being 424 mm. Moreover, since the two quadrupoles at the Q1 location are not parallel to each other, the separation (and hence the amount of cross talk) between them is different at the two ends of these magnets. The non-allowed harmonics (in particular  $b_o$ , which is affected the most) are a maximum when the separation between the two quadrupoles is a minimum. The results of calculations for this case using the code POISSON are given in Table 6.3.4. The maximum operating current in the present design is about 5.05 kAmp. The amount of cross talk is negligible in the design range of operation and is very small up to the expected quench current (8.26 kA). The field lines at quench in one of two side-by-side quadrupoles are shown in Fig. 6.3.5 (the other quadrupole, not shown, is on the left side of the one shown).

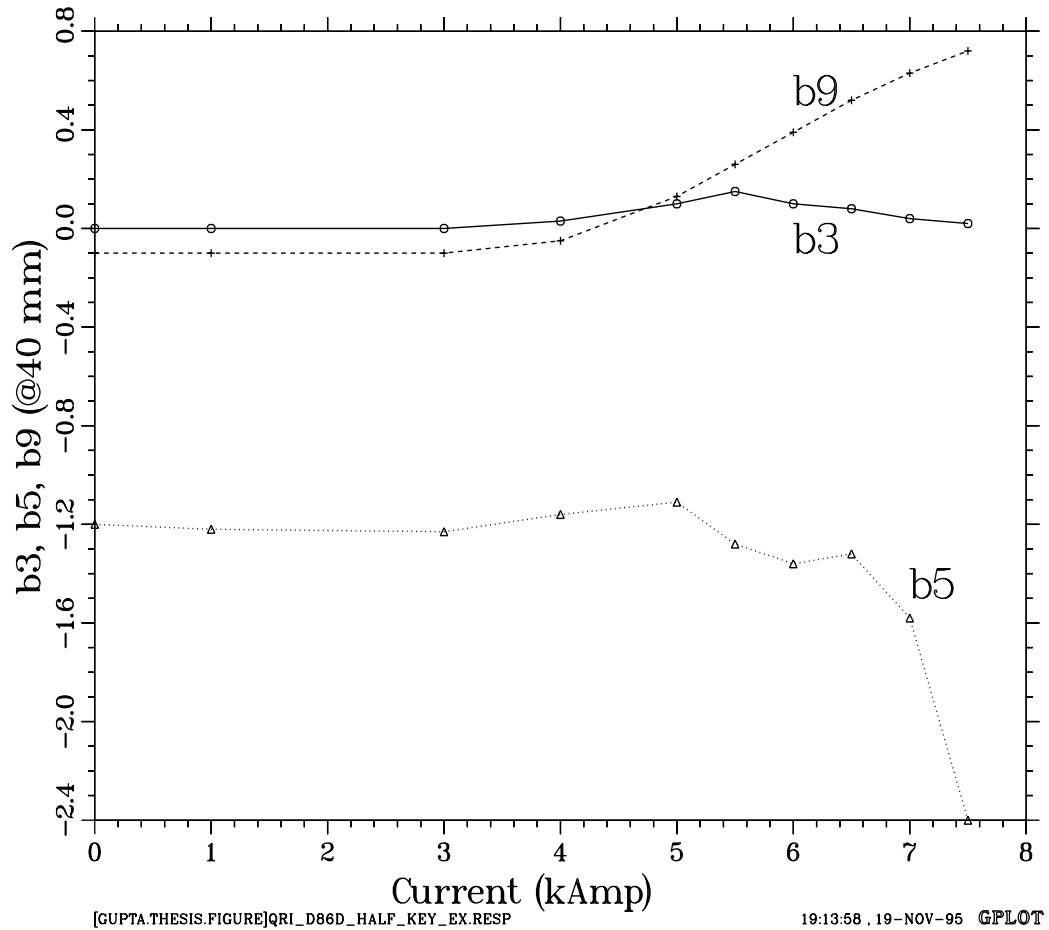


**Figure 6.3.4:** Variation in the  $b_3$ ,  $b_5$  and  $b_9$  harmonics as a function of current in 130 mm aperture RHIC insertion quadrupole as computed with the code POISSON. The computer model is shown in Fig. 6.3.3.

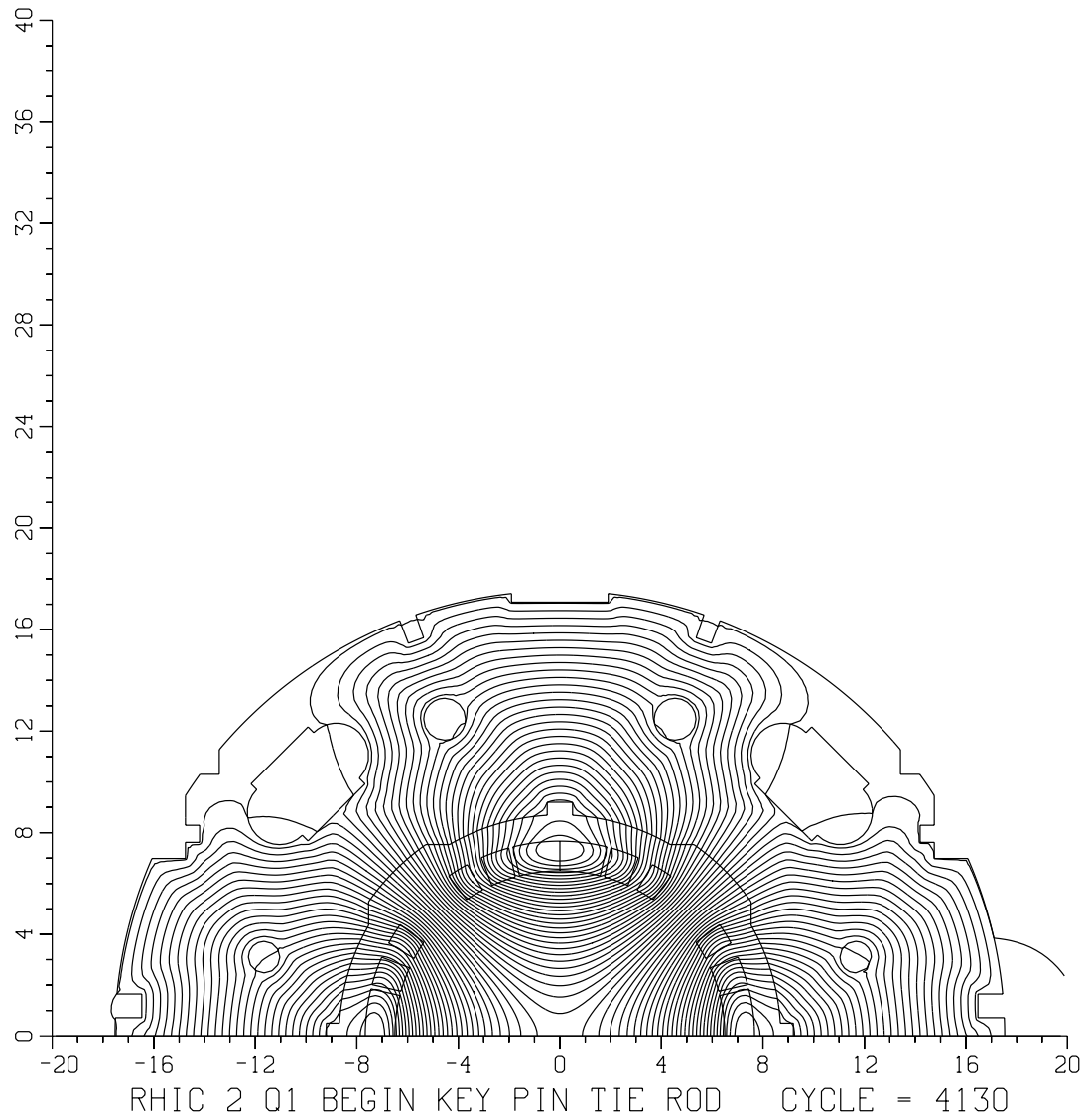


**Figure 6.3.5:** The field lines at quench in one of two side-by-side quadrupoles. The other quadrupole, not shown, is on the left side of the one shown. The minimum center to center distance between the two quadrupoles is 42.4 cm.

**Table 6.3.4:** Harmonics in the straight section of the RHIC 130 mm aperture quadrupoles at the Q1 location where the separation between the two side-by-side quadrupoles is a minimum (424 mm). The harmonics are given at 40 mm radius.  $\infty\mu$  represents the calculations when the permeability in the iron is assumed to be  $\infty$ . *Grad* denotes the field gradient. These computations are made using the code POISSON.

I	<i>Grad</i>	T.F.	$b_0$	$b_2$	$b_3$	$b_4$	$b_5$	$b_6$	$b_7$	$b_8$	$b_9$
kAmp	T/M	T/M/kA	$10^{-4}$	$10^{-4}$	$10^{-4}$	$10^{-4}$	$10^{-4}$	$10^{-4}$	$10^{-4}$	$10^{-4}$	$10^{-4}$
$\infty\mu$	$\infty\mu$	9.5742	0.00	0.00	0.00	0.00	-1.20	0.00	-0.10	0.00	0.00
1.0	9.5735	9.5735	-0.03	0.01	0.01	0.01	-1.22	0.01	-0.10	0.00	0.00
3.0	28.7171	9.5724	-0.03	0.02	0.00	0.01	-1.23	0.01	-0.10	0.00	0.00
4.0	38.2591	9.5648	0.14	0.02	0.07	-0.02	-1.16	0.01	-0.11	0.01	0.05
5.0	47.6671	9.5334	0.14	0.01	0.05	-0.02	-1.09	0.01	-0.11	0.01	0.24
5.5	52.2588	9.5016	0.14	0.07	0.05	-0.02	-1.25	0.01	-0.12	0.00	0.37
6.0	56.7113	9.4519	0.25	0.08	0.03	-0.01	-1.33	0.01	-0.13	0.01	0.50
6.5	61.0000	9.3846	0.13	0.03	0.01	0.01	-1.31	0.01	-0.14	0.01	0.63
7.0	65.1185	9.3026	0.42	0.05	-0.02	0.02	-1.60	0.01	-0.15	0.01	0.74
7.5	69.0458	9.2061	0.82	0.09	-0.01	0.04	-2.44	0.01	-0.15	0.01	0.83
8.0	72.8246	9.1031	1.61	0.19	-0.16	0.07	-3.74	0.02	-0.17	0.01	0.89
8.5	76.5132	9.0016	2.78	0.32	-0.47	0.12	-5.27	0.03	-0.19	0.01	0.93
9.0	80.1467	8.9052	4.06	0.46	-0.73	0.17	-6.84	0.03	-0.21	0.01	0.97
9.5	83.7381	8.8145	5.53	0.59	-0.87	0.22	-8.40	0.04	-0.21	0.01	0.990

#### 6.3.4. Expected Quench Performance

To compute the gradient at quench, the maximum field on the conductor (the peak field) is first calculated. The location of the peak field is on the pole-most surface of the pole turn. It is 16% radially outward from the coil inner radius. The value of this field together with the gradient at 7000 A and 8000 A is given in Table 6.3.5.

**Table 6.3.5:** Peak field on the cable in the 130 mm aperture quadrupole. The peak field in the coil is on the pole turn.

Current	Gradient	Field
7000 A	65.07 T/m	4.991 T
8000 A	73.16 T/m	5.626 T

The specification for the critical current in the wire is  $\geq 286$  amperes at 4.2 K temperature and 5 Tesla field. In this 36 strand cable, after a 2% degradation, the minimum critical current in the cable is specified to be 10,100 amperes. This gives a computed quench gradient of 75.3 T/m at 4.6 K, which is 57% over the design value of 48.1 T/m. The computed quench current is 8260 amperes which is  $\sim 64$  % above the design value of 5050 amperes. The current density in the copper at quench is 1133 A/mm<sup>2</sup> and at design field is about 670 A/mm<sup>2</sup>. The critical current in the cable actually used in manufacturing the magnets is about 12,000 ampere, which is much better than the minimum specified value. This would give a quench gradient of 80.1 T/m and quench current of 8860 ampere.